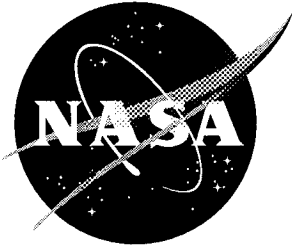


108532  
C2/15

# Modeling of Rolling Element Bearing Mechanics—Computer Program Updates

---

*S.G. Ryan*



# Modeling of Rolling Element Bearing Mechanics—Computer Program Updates

---

S.G. Ryan  
*Marshall Space Flight Center • MSFC, Alabama*

National Aeronautics and Space Administration  
Marshall Space Flight Center • MSFC, Alabama 35812

---

March 1997



## TABLE OF CONTENTS

|   | Page |
|---|------|
| INTRODUCTION .....  | 1    |
| THEORETICAL MANUAL UPDATES .....                            | 1    |
| Solution Methodology (Section 2.1) .....                    | 1    |
| Constraints and Solution Procedure (Sections 7.1–7.3) ..... | 2    |
| Programming Implementation (Section 8) .....                | 6    |
| USER’S MANUAL UPDATES .....                                 | 13   |
| Effects of Functional Changes .....                         | 14   |
| Effects of Theoretical Changes .....                        | 18   |
| Additional User’s Manual Changes .....                      | 20   |
| GENERAL COMMENTS ON ASSUMPTIONS AND INHERENT ERRORS .....   | 21   |
| APPENDIX .....  | 23   |

## LIST OF ILLUSTRATIONS

| Figure | Title  | Page |
|--------|--|------|
| 1a.    | FEREBA subroutine calling tree .....                         | 8    |
| 1b.    | FEREBA subroutine calling tree (continued) .....             | 9    |
| 1c.    | FEREBA subroutine calling tree (continued) .....             | 10   |
| 2.     | FEREBA flow chart .....                                      | 11   |
| 3.     | UPDATE flow chart .....                                      | 12   |
| 4.     | Overall schematic of REBANS operation .....                  | 13   |
| 5.     | Example force/deflection curve .....                         | 15   |
| 6.     | Gap 2 constraint forces for ball locations 1, 2, and 3 ..... | 16   |
| 7.     | Outer race curvature center deflections polar plot .....     | 17   |
| 8.     | Example of FEREBA status information output .....            | 19   |

## **TECHNICAL MEMORANDUM**

# **MODELING OF ROLLING ELEMENT BEARING MECHANICS— COMPUTER PROGRAM UPDATES**

## **INTRODUCTION**

The Rolling Element Bearing Analysis System (REBANS) was developed for NASA's Marshall Space Flight Center (MSFC) by Aerojet. The initial version (version 1.10), delivered in December 1994, contained several errors and exhibited numerous convergence difficulties. The program has been modified in house at MSFC to correct the errors and greatly improve the convergence (version 2.0). The most significant changes are related to the improved convergence and will be described in the Solution Methodology section and the Constraints and Solution Procedure section. The other changes, corrections, and enhancements will be discussed in the Programming Implementation section.

## **THEORETICAL MANUAL UPDATES**

The changes affecting convergence address areas discussed in sections 2.1, 7, and 8 of the original Theoretical Manual. In this discussion, equations and figures in the original manual will be referenced by the original numbers, preceded by an uppercase letter "A." The original nomenclature will be used, as well. Many aspects of the original theory remain applicable after the changes; therefore, the reader should be familiar with the initial theory before examining the updates.

The introductory material of section 7 (pages 7-1 through the beginning of 7-3) remains valid. Likewise, sections 7.4 and 8.4 remain valid. The material which follows modifies the remainder of sections 2.1, 7, and 8.

### **Solution Methodology (Section 2.1)**

The program can operate in two modes. The primary mode is to accept user-specified shaft/inner race displacements and calculate the resulting loads. The other mode is to accept forces and moments as input and determine the corresponding shaft/inner race displacements. This mode is essentially the first mode with an outer iteration loop around it.

For either of the solution modes described above, the fundamental problem to be solved is this: given a position of the shaft/inner race, determine rolling element positions and loads and race elastic deflections. The resulting rolling element loads are then summed to yield the net forces and moments on the shaft. This fundamental problem is the area addressed by the changes.

The original approach utilized sequential convergence of nested loops to achieve final convergence. This approach proved to be seriously deficient in robustness. Convergence was more the exception than the rule. The approach was changed to iterate all variables simultaneously. This has the advantage of using knowledge of the effect of each variable on each other variable (via the system Jacobian) when determining the incremental changes. The steps are as follows:

1. The outer ring is fixed at its current position (begins at initial guess). The inner race is at a prescribed position. Using classical quasi-static analysis procedures, the rolling element positions and loads are determined.
2. Calculated loads are applied to the outer and inner races and elastic deflections calculated. Nonlinear gap closures are identified and constraint forces determined. The constraint forces are now modeled using artificial, stiff springs at closed gaps. The partial derivatives of rolling element and constraint forces with respect to race elastic deflections are determined using finite perturbations. These data are used to calculate incremental changes in race elastic deflections. This process is repeated until convergence is attained.
3. If the program is running in the force input mode, a series of inner race displacement perturbations is made in order to calculate the partial derivatives of forces and moments with respect to inner race displacements. These data are used to calculate increments in the inner race displacements, and the process is repeated until convergence is achieved.

### **Constraints and Solution Procedure (Sections 7.1–7.3)**

The original approach to defining constraint forces was to force gap deflections to identically equal clearances at locations where contact occurs. For a given set of assumed closure locations, the contact forces required to enforce the constraints can be calculated as described in section 7.3. The difficulty with this approach is that the calculated constraints then change the race deflections and generate a new set of closure locations. This requires an iterative solution for each stage of the larger iteration loop involving rolling element forces. The current approach treats the contact forces using artificial stiff springs.

The formulation begins using equation (A7–2) and augmenting it with the corresponding equation for the inner race, yielding:

$$\begin{Bmatrix} U_{1o} \\ U_3 \\ U_{1i} \end{Bmatrix} = \begin{bmatrix} CO_{12}^o & CO_{13}^o & 0 \\ CO_{32}^o & CO_{33}^o & 0 \\ 0 & 0 & CO_{12}^i \end{bmatrix} \begin{Bmatrix} F_{bo} \\ F_c \\ F_{bi} \end{Bmatrix} \quad (1)$$

The subscripts and superscripts  $o$  and  $i$  have been added to refer to the outer and inner race, respectively. The outer race rolling element force vector is a function of both the inner and outer race curvature center deflections:

$$F_{bo} = F_{bo} (U_{1o}, U_{1i}) \quad (2)$$

The inner race rolling element force vector is a function of both, as well:

$$F_{bi} = F_{bi} (U_{1o}, U_{1i}) \quad (3)$$

The outer race constraint force vector is a function only of the deflections of potential contact points on the outer race and carrier:

$$F_c = F_c (U_3) = \begin{cases} -K_{\text{contact}} (U_{3\text{race}} - U_{3\text{carrier}} - \text{clearance}) & ; \text{for closed gaps} \\ 0 & ; \text{for open gaps} \end{cases} \quad (4)$$

where  $K_{\text{contact}}$  is set to a value much larger than any actual stiffness in the system. In terms of the gap variable defined in equation (A7-9) (equation (A7-14) for negative faces), equation (4) for closed gaps becomes:

$$F_{c_k} = K_{\text{contact}} (U_3(C_k) + G_k - U_3(O_k)) = K_{\text{contact}} \Delta g(k) \quad (5)$$

Equation (1) can be written more concisely as

$$\mathbf{U} = \mathbf{CF}(\mathbf{U}) \quad (6)$$

This implicit equation can be iteratively solved using Newton's method. Applying a first order perturbation to equation (6) yields:

$$\mathbf{U}_0 + \delta\mathbf{U} \approx \mathbf{CF}(\mathbf{U}_0) + \mathbf{C} \left[ \frac{\partial \mathbf{F}}{\partial \mathbf{U}} \Big|_{\mathbf{U}_0} \right] \delta\mathbf{U} \quad (7)$$

which can be rearranged to:

$$\left[ \mathbf{I} - \mathbf{C} \frac{\partial \mathbf{F}}{\partial \mathbf{U}} \Big|_{\mathbf{U}_0} \right] \delta\mathbf{U} \approx \mathbf{CF}(\mathbf{U}_0) - \mathbf{U}_0 \quad (8)$$



Equation (8) now forms the basis for the iterative solution. Substituting the  $n^{\text{th}}$  iterate for the equilibrium value (subscript 0) results in:

$$\left[ \mathbf{I} - \mathbf{C} \frac{\partial \mathbf{F}}{\partial \mathbf{U}} \bigg|_{\mathbf{U}_n} \right] \delta \mathbf{U}_n = \mathbf{C} \mathbf{F}(\mathbf{U}_n) - \mathbf{U}_n = \mathbf{R}_n \quad (9)$$

where  $\mathbf{R}_n$  is the residual vector which should ideally be zero when a solution is found. The Jacobian  $\left( \frac{\partial \mathbf{F}}{\partial \mathbf{U}} \right)$  and the residual must be evaluated at every iteration point. Once this is done, equation (9) can be solved for  $\delta \mathbf{U}_n$  using standard linear algebra techniques. Convergence is achieved when the error norm, defined by:

$$err_n = \frac{\|\mathbf{R}_n\|}{\|\mathbf{U}_n\|} \quad (10)$$

is less than a specified tolerance.

Equation (9) can be expanded to the notation of equation (1) yielding:

$$\begin{aligned} & \left[ \mathbf{I} - \begin{bmatrix} CO_{12}^o & CO_{13}^o & 0 \\ CO_{32}^o & CO_{33}^o & 0 \\ 0 & 0 & CO_{12}^i \end{bmatrix} \begin{bmatrix} \frac{\partial F_{bo}}{\partial U_{1o}} & 0 & \frac{\partial F_{bo}}{\partial U_{1i}} \\ 0 & \frac{\partial F_c}{\partial U_3} & 0 \\ \frac{\partial F_{bi}}{\partial U_{1o}} & 0 & \frac{\partial F_{bi}}{\partial U_{1i}} \end{bmatrix} \bigg|_{\mathbf{U}_n} \right] \begin{Bmatrix} \delta U_{1o} \\ \delta U_3 \\ \delta U_{1i} \end{Bmatrix}_n \\ &= \begin{bmatrix} CO_{12}^o & CO_{13}^o & 0 \\ CO_{32}^o & CO_{33}^o & 0 \\ 0 & 0 & CO_{12}^i \end{bmatrix} \begin{Bmatrix} F_{bo} \\ F_c \\ F_{bi} \end{Bmatrix} \bigg|_{\mathbf{U}_n} - \begin{Bmatrix} U_{1o} \\ U_3 \\ U_{1i} \end{Bmatrix}_n \end{aligned} \quad (11)$$

The solution estimates are updated as follows:

$$\begin{Bmatrix} U_{1o} \\ U_3 \\ U_{1i} \end{Bmatrix}_{n+1} = \begin{Bmatrix} U_{1o} \\ U_3 \\ U_{1i} \end{Bmatrix}_n + \begin{Bmatrix} \delta U_{1o} \\ \delta U_3 \\ \delta U_{1i} \end{Bmatrix}_n \quad (12)$$

The process is repeated until convergence is attained.

Examination of equation (11) reveals that there are two types of partial derivative evaluations required. The first is the partial of inner and outer race rolling element forces with respect to inner and outer race curvature center elastic deflections. These partials are determined by numerically perturbing each curvature center variable independently and forming finite difference approximations to the partial derivatives. The second is the partial of the constraint force with respect to deflections of the outer race and carrier gap variables. It can be seen from equation (5) that, for closed gaps, this partial is simply  $K_{\text{contact}}$  with the appropriate sign based on whether the face is positive or negative and whether the variable is on the race or the carrier. For open gaps, it must first be determined whether the gap corresponds to an unloaded preload spring. This is correctly addressed in section 7.4. If the gap does not correspond to an unloaded preload spring, the partial is zero. If it does, the partial is equal to  $K_{\text{prei}}$  (equation (A7–21)) with the appropriate sign based on whether the face is positive or negative and whether the variable is on the race or the carrier.

## Programming Implementation (Section 8)

This section will describe the program logic and subroutine hierarchy required to implement the previously defined theory. In addition to the theoretical changes discussed, some additional functional and minor theoretical changes have been made in the implementation:

1. FEREBBA will now write the reduced flexibility matrices to a disk file. This enables the user to make subsequent analyses which use the same race model without having to recompute these matrices.
2. For the displacement input mode, multiple sets of inner ring displacements can be read from a file. These will be solved sequentially. The initial guess for a new solution set will be the solution values from the previous set. This facilitates the determination of load-deflection curves for a bearing.
3. The displacement input mode can be run with force iteration in the axial direction only. This allows the user to specify a fixed axial load while determining the reactions to the lateral displacements and rotations. This is also useful to determine the initial axial displacement needed to yield a certain initial preload for the more typical displacement input mode. This feature is primarily useful for simplex bearing arrangements.
4. FEREBBA will calculate an average "rigid body" tilt for the outer ring based on weighted averages of the elastic deflections of the finite element model node locations.
5. Several additional output files are now generated for each run. For the multiple case displacement input, the displacements and loads are written in a tabular format to an ASCII file and to a binary file. These files facilitate interpretation and plotting of results. The outer ring constraint forces are also written to a binary file. In addition, the capability has been added to graphically display the outer race curvature center (ORCC) deflections as a distorted ring. The values defining these curves are written to another binary file for plotting.
6. For simplex bearing configurations, the user can specify a lateral stiffness between the race and carrier at the preload spring contact face. This is used to represent the lateral load path which can occur due to friction between the spring and the carrier and race axial faces.
7. A set of external forces can be applied to the outer race independently of the preload and internal reaction forces. One interesting use of this capability is to apply a moment to force the race to cock or tilt within the deadband resulting in "corner-to-corner" deadband contact or gap closure. This would be used to partially simulate a cocked and hung bearing. Since friction forces are not included, the race would still be free to slide axially.
8. The original code required two radial master degrees-of-freedom (DOF's) on the outer diameter of the outer race. This introduced a significant error due to the large spatial resolution in the axial

direction. The code has been changed to require three radial master DOF's on this surface. This allows for "corner" nodes to properly carry tilt loads and a central node to account for "bridging" of the race. The bearing support configuration descriptions in section 3.1 of the Theoretical Manual have been applied updated for cases affected by this change (IBSCOR=2, 3, 5, 6, 8, 9). These updates are included in the appendix.

9. With the new solution approach, an initial guess (call to subroutine INDEL) must be made for the outer race deflections, even in the displacement input mode.
10. The constraint transformation matrices  $T_s$  defined in equation (A7-17) and  $T_f$  defined in equation (A7-20) provide notational convenience but are computationally inefficient. A more efficient implementation has been applied that uses index arrays and indirect addressing of array components to perform the same functions.
11. Duplex bearing analysis previously required an ANSYS model of the inner race-shaft in order to determine initial offsets needed for a specified preload. A subroutine has been added (CIRIG) that generates an inner race compliance matrix corresponding to two rigid rings connected by "pseudorigid" (i.e., very stiff) springs. This allows duplex bearing analysis without requiring a full finite element model of the inner race.
12. For duplex bearing analysis, there was previously a convergence error in the iterative calculation of the preload induced contact angle (equation (A5-32)). This value is used in the calculation of the preload-induced axial elastic displacement of the inner rings (equation (A5-35)). The function,  $f(\alpha_p)$ , and its derivative,  $f'(\alpha_p)$ , contain a singularity at the value  $\alpha_p = \alpha^\circ$ . The original approach used  $\alpha^\circ$  as the initial guess for the iteration and, consequently, it never converged. The initial guess was modified to  $1.1\alpha^\circ$  to avoid this singularity. Starting at a value greater than  $\alpha^\circ$  is appropriate since axial preload will always increase the angle from its unloaded value.
13. The rolling element orbital speed used in the centrifugal force calculation was based on the initial estimate of rolling element positions from subroutine GUESS. The algorithm has been revised to update the speeds based on the positions obtained from an initial solution by DNEQNF (same as the original final solution). With the updated orbital speeds (and resulting centrifugal forces), DNEQNF is called again to yield a revised solution. This process could theoretically be iterated until convergence is achieved; however, the speed change was found to be insignificant after only one update so no looping logic was coded.

The subroutine calling hierarchy is shown in figures 1a through 1c. The subroutines listed in bold type are newly created to implement the program changes. The subroutines listed in italic type are not used by FEREB A but are included for anticipated future functionality. The logic flow is presented in the flow chart of figures 2 and 3. Figure 2 is the overall program flow chart and figure 3 is the flow chart for the UPDATE subroutine. The variable list of section 8.4 in the original manual remains valid.

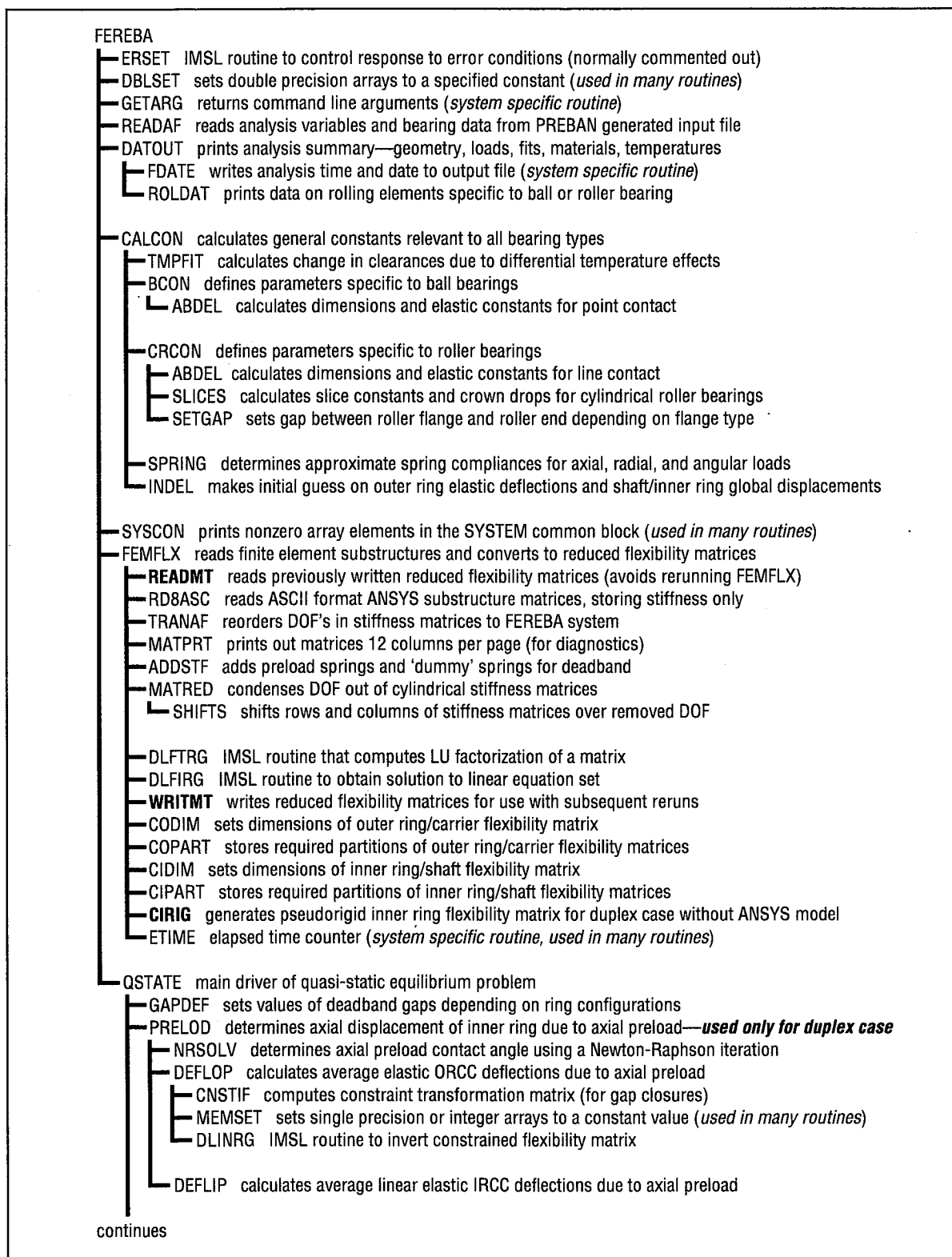
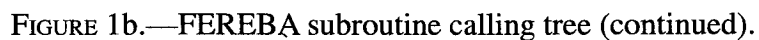


FIGURE 1a.—FEREBA subroutine calling tree.



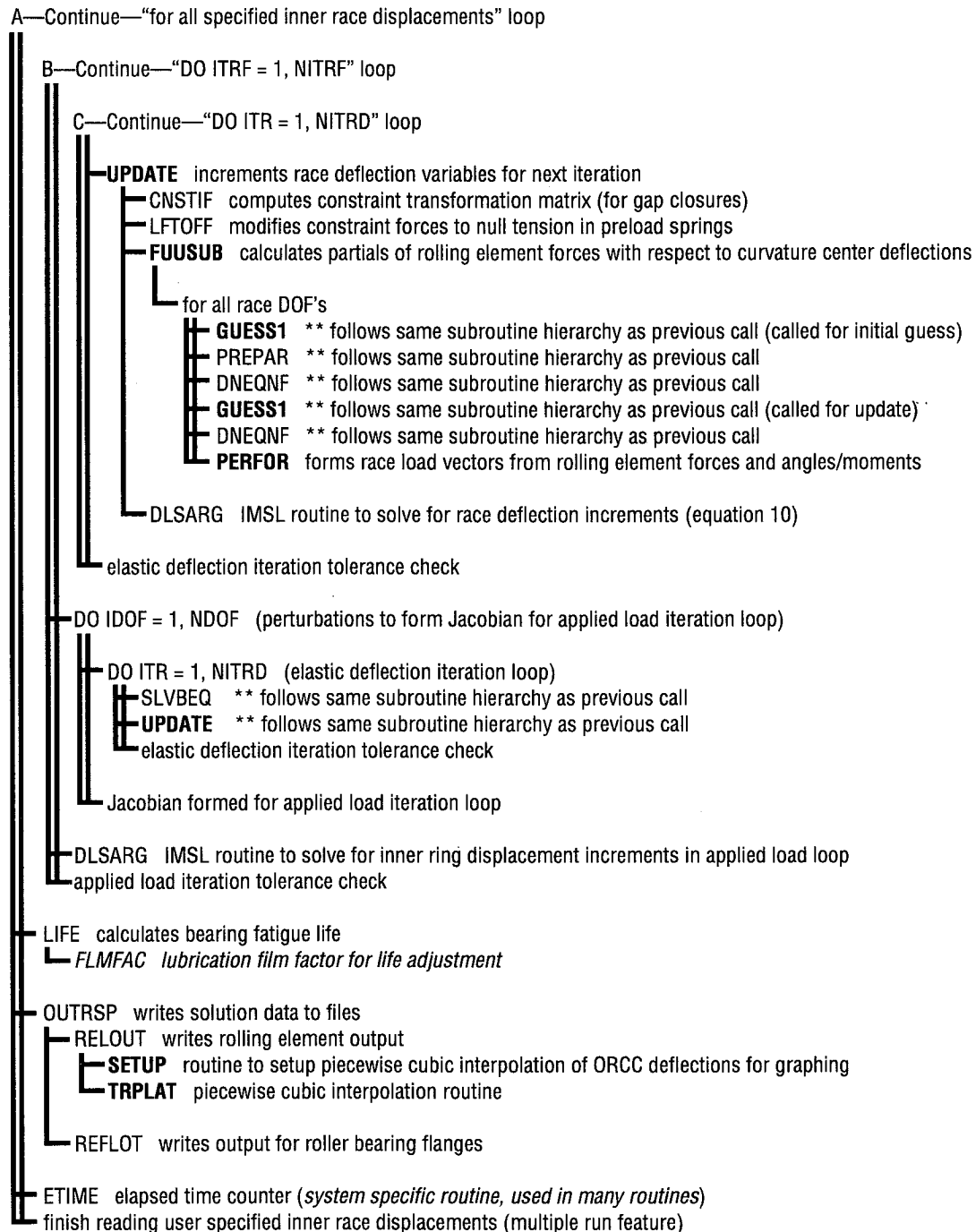


FIGURE 1c.—FEREBA subroutine calling tree (continued).

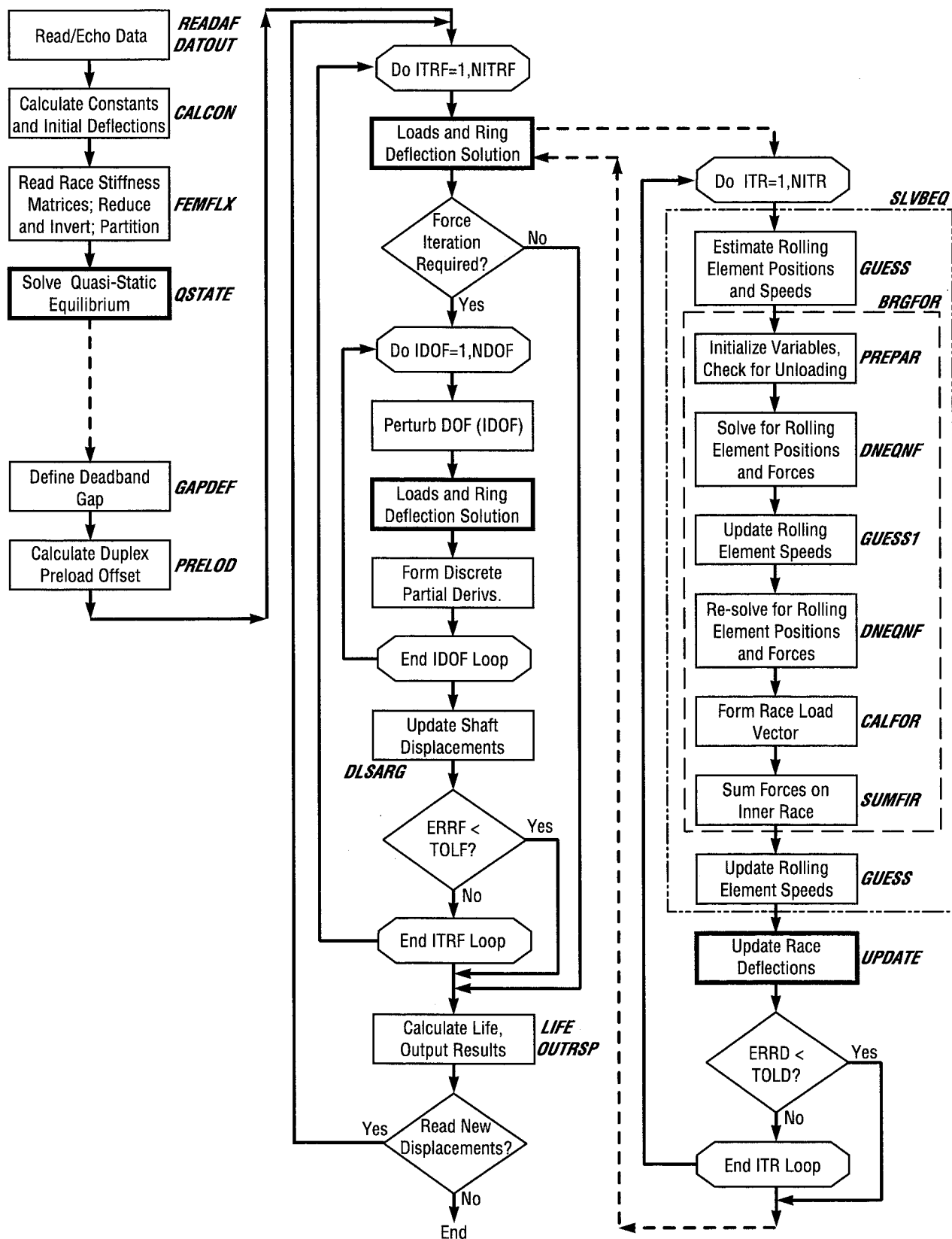


FIGURE 2.—FEREBA flow chart.



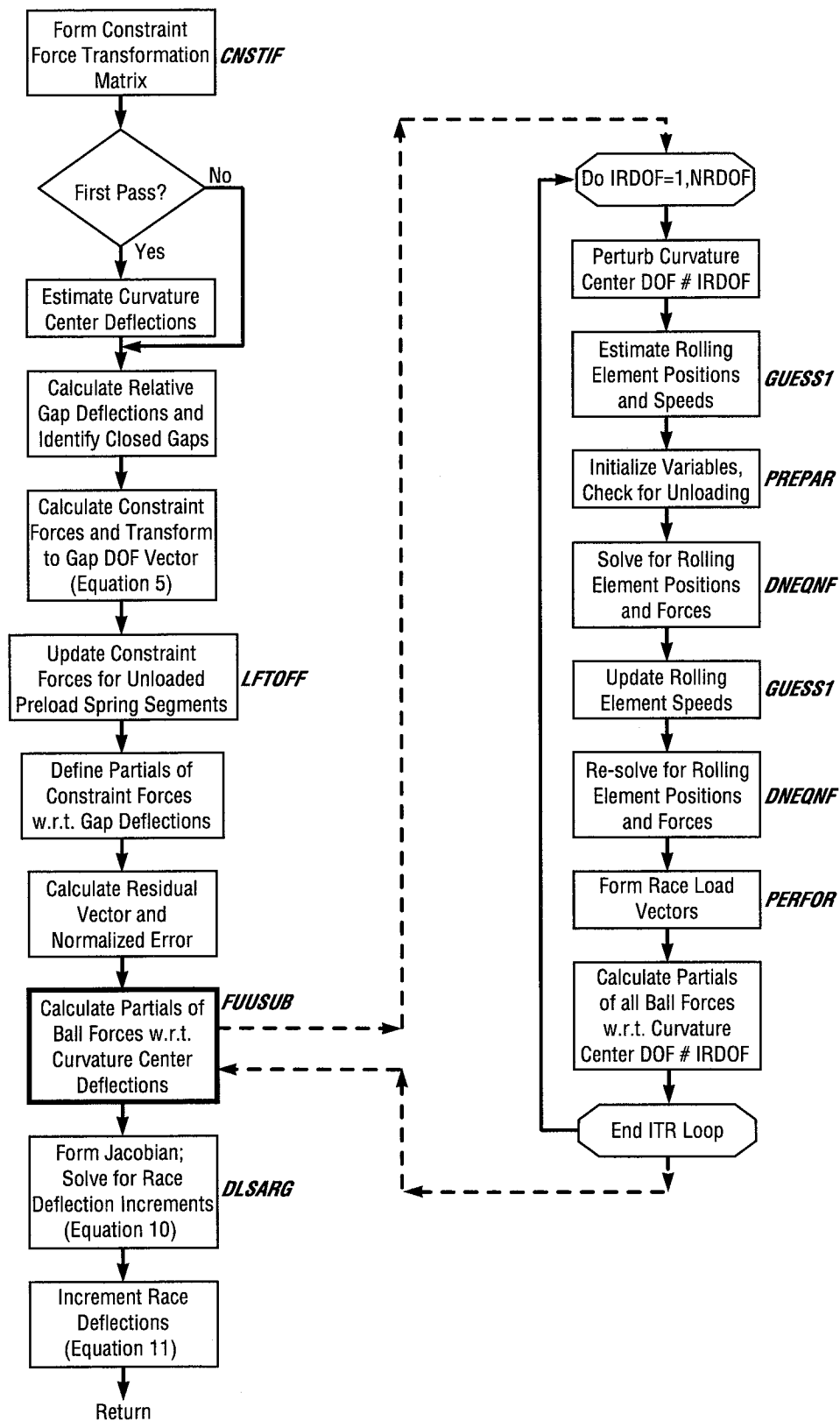


FIGURE 3.—UPDATE flow chart.

## USER'S MANUAL UPDATES

The theoretical and functional changes described in the previous section impact the user primarily through additional input and output files. This is illustrated in the revised schematic of figure 4 (replaces fig. A2-1). The additional files are the result of the functional changes rather than the theoretical changes. The theoretical changes alter some of the output in the existing output file. These effects will be discussed later. The modifications and additional files required/generated by the functional changes will be discussed first. These will be referenced to the numbering used in the Programming Implementation subsection of the Theoretical Manual Updates section.

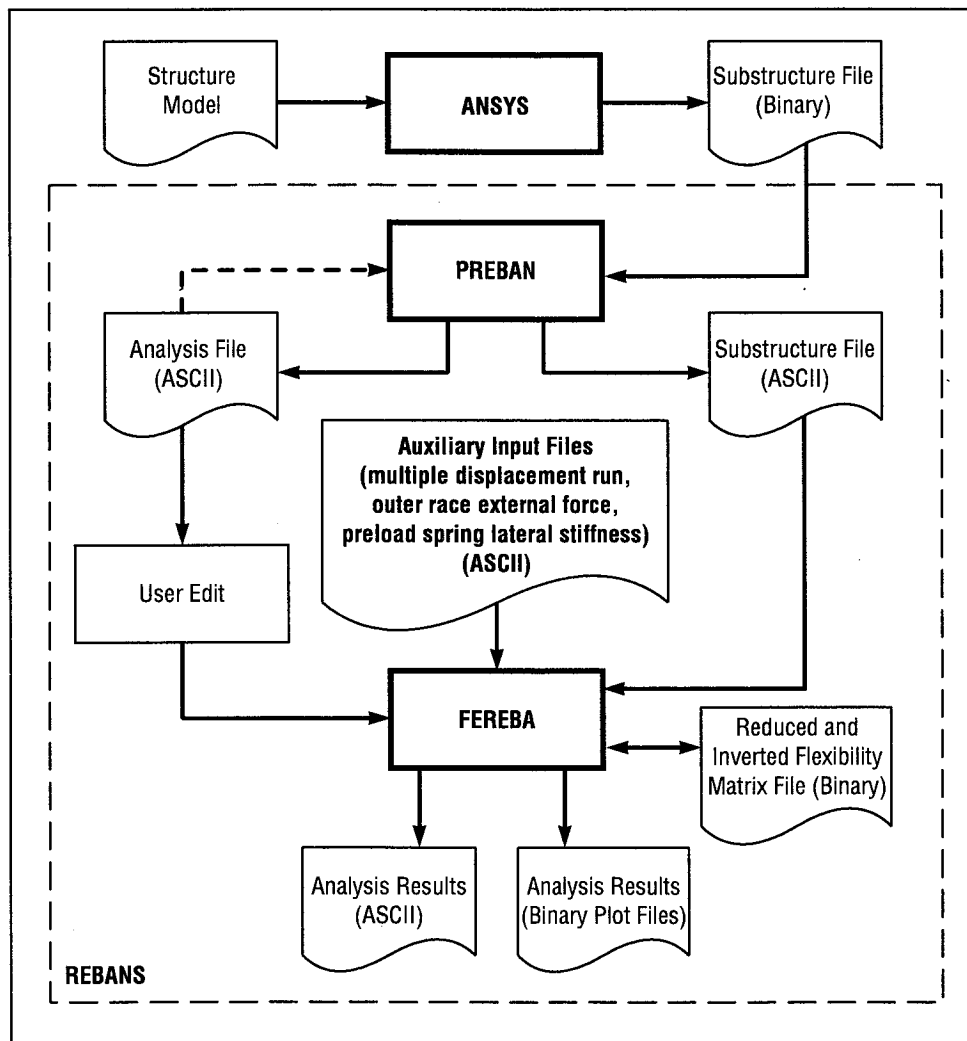


FIGURE 4.—Overall schematic of REBANS operation.

## Effects of Functional Changes

1. FEREBABA will write the reduced flexibility matrices to a file whose name is based on the original substructure file name. The name is generated by prefixing the original substructure file name with "red." to signify that it contains the "reduced" flexibility matrices. If FEREBABA finds a file by this name it will use it instead of reading the substructure file and reducing and inverting the stiffness matrix; therefore, if changes are made to the ANSYS model and the same file name is used, the "red.\*" file must be moved or deleted. This file also contains the axial preload spring stiffness so that if it is changed in the analysis file the substructure file will be reread and reduced. If the user attempts to add or change a lateral preload spring stiffness (functional change 6), the change will not be recognized since FEREBABA will read the reduced flexibility matrices rather than the substructure stiffness matrix.
  
2. The multiple sets of inner ring displacements are supplied by the user in an ASCII file read from FORTRAN unit number 51. Each record of this file should contain four comma-separated values. These values correspond to: Y-Axis Translation, Z-Axis Translation, XZ-Plane Rotation (About Y), XY-Plane Rotation (About Z). Multiple axial displacements are not currently provided for. Each case will be solved sequentially until an end-of-file is reached. The file will be read if appropriate linkage exists between it and FORTRAN unit number 51 (procedures for connecting a file to a FORTRAN unit number are operating system-dependent). If the program is running in force input mode, this file is ignored.
  
3. In order to run the displacement input mode with force iteration in the axial direction only, the user must edit the analysis file (\*.dat). Beginning with an analysis file that is set up for displacement input mode, insert a "LOADS" set immediately prior to the "DISPL" data. This set should contain the desired axial preload in the first record and zero for the remaining four records. The axial translation in the "DISPL" set will be ignored. For example, the records

### LOADS

|               |               |
|---------------|---------------|
| 1000.0000E+00 | preload force |
| 0.0000000E+00 |               |
| 0.0000000E+00 |               |
| 0.0000000E+00 |               |
| 0.0000000E+00 |               |

### DISPL

|               |                             |
|---------------|-----------------------------|
| 0.0000000E+00 | X-Axis (Axial) Translation  |
| 2.2000000E-03 | Y-Axis Translation          |
| 0.0000000E-03 | Z-Axis Translation          |
| 0.0000000E-07 | XZ-Plane Rotation (About Y) |
| 0.0000000E-07 | XY-Plane Rotation (About Z) |

will iterate axial translation to achieve 1,000 pounds of axial load while the Y-axis translation is fixed at 0.0022 inch.

4. The calculated average "rigid body" tilt for the outer ring is written to the ASCII output file and to an additional binary file for plotting (see item 5).
5. The displacements and loads for the multiple displacement cases are written to FORTRAN unit number 62 with a binary write and to unit number 61 with a free format write. Each record is structured as follows:

$$X, F_{sum_x}, Y_{avg}, F_{sum_y}, Z_{avg}, F_{sum_z}, \Theta_{avg_y}, M_{sum_y}, \Theta_{avg_z}, M_{sum_z},$$

$$(Tilt_i, i = 1, nbrg), (F_x, F_y, F_z, M_y, M_z)_i, i = 1, nbrg.$$

The *sum* and *avg* subscripts refer to summing and averaging values for both bearings of a duplex set. The designation *nbrg* is 2 for a duplex bearing and 1 otherwise. Figure 5 shows an example plot from this file. The outer ring constraint forces are written to FORTRAN unit number 64 with a binary write. Each record is structured as follows:

$$Y_{avg}, Z_{avg}, \Theta_{avg_y}, \Theta_{avg_z}, F_{c_i}, i = 1, \text{number of gaps}.$$

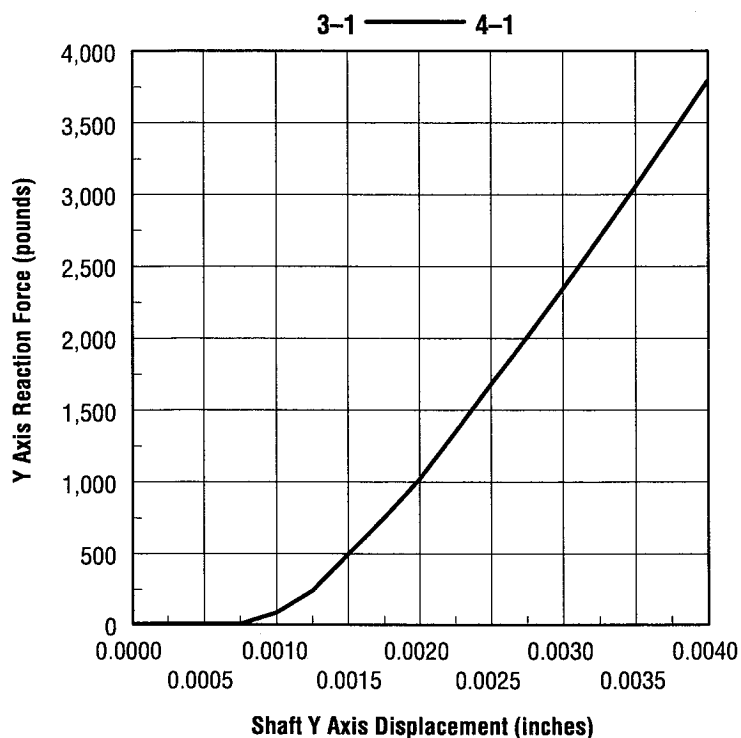


FIGURE 5.—Example force/deflection curve.

Figure 6 shows an example plot from this file. The polar plot for the ORCC deflections is written to FORTRAN unit number 63 with a binary write. Each record is structured as follows:

$$y^* + \Delta_{y_1}, z^* + \Delta_{z_1}, y^*, z^*, y^* + \Delta_{y_2}, z^* + \Delta_{z_2}.$$

The values of  $y^*$  and  $z^*$  correspond to a circle with a radius of 2.5 times the radial gap value. The subscripts 1 and 2 refer to bearings 1 and 2 in a duplex set (if it is duplex). The  $y$  axis deflection of the race at ball position 1 has been subtracted from the values of  $\Delta_{y_1}$  to remove the "rigid body" translation bias from the plot (for loading in the  $+y$  direction). This facilitates the comparison of the deflected plot with the undeflected plot. Figure 7 shows an example plot from this file. The dotted line represents the undeflected plot and the solid line the deflected plot. For multiple displacement cases this plot is of marginal utility. Each successive deflected ring is drawn over the previous ones so that the deflected shapes are usually not visible.

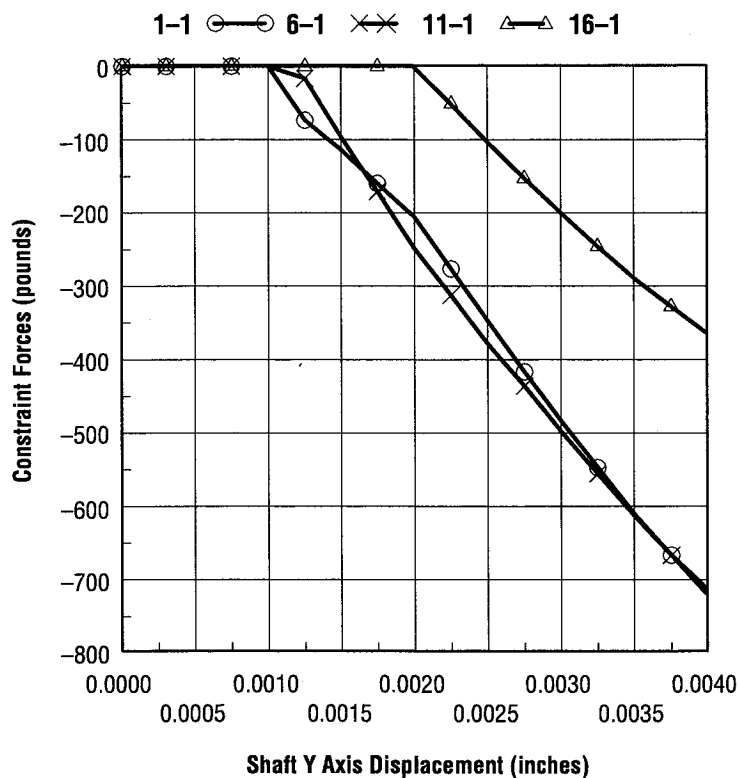


FIGURE 6.—Gap 2 constraint forces for ball locations 1, 2, and 3.

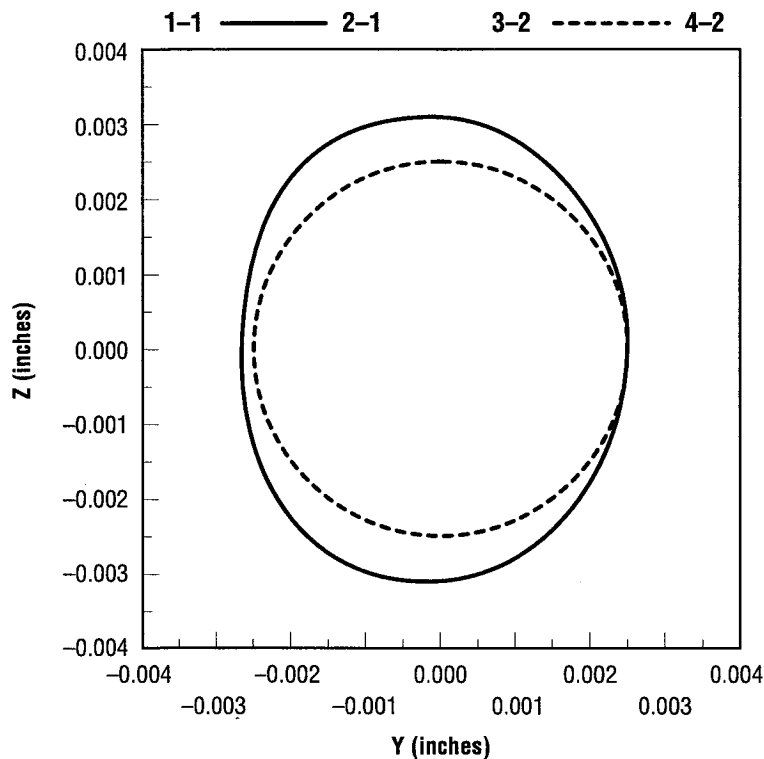


FIGURE 7.—Outer race curvature center deflections polar plot.

6. The lateral stiffness between the race and carrier at the preload spring contact face is supplied by the user in an ASCII file read from FORTRAN unit number 53. This value should be on the first record beginning in the first column.
7. The set of external forces applied to the outer race are supplied by the user in an ASCII file read from FORTRAN unit number 52. The number of such forces must be the only value on the first record (beginning in the first column) of this file. Each remaining record should contain two comma-separated values. The first value is an integer number designating the gap DOF index number corresponding to the location of force application. The second value is the force magnitude at that location. As an example, for IBSCOR=2 with 11 balls, the records

3  
1,500.  
26,-250.  
31,-250.

will apply 500 pounds in the axial direction at ball location 1 and -250 pounds in the axial direction at each of ball locations 6 and 7. To determine the gap DOF numbering the user must refer to the appendix (revises section 3 of the original Theoretical Manual due to the additional radial master DOF).

8. The additional radial master DOF requires a change to the ANSYS model. The outer race configuration descriptions of section 3.2 of the User's Manual should be modified according to the Theoretical Manual updates provided in the appendix. The example ANSYS input file of section 3.4 should be modified where the master DOF's are defined. Lines 240 and 241 should be replaced with the following:

|                                |                                     |
|--------------------------------|-------------------------------------|
| M, 1023, UX, 1029, 6, UY, UZ   | * Master nodes 1023 and 1029        |
| MGEN, NRE, MINC, 1023, 1029, 6 | * Define similar nodes as masters   |
| M, 1024, UX, 1028, 2, UY, UZ   | * Master nodes 1024, 1026, and 1028 |
| MGEN, NRE, MINC, 1024, 1028, 2 | * Define similar nodes as masters.  |

Similar changes should be made to models of other configurations.

### Effects of Theoretical Changes

The changes made in the theoretical development only affect the program output. This occurs primarily in the definition of "error" and in the messages related to convergence failure. Due to the new iteration approach, the error norm (defined by equation (9)) is no longer an "average" of various displacement errors as before. There are also no longer separate errors for the inner and outer races. Deflection errors for both races are contained in the residual vector  $\mathbf{R}_n$ . Referring to the User's Manual, this will change the sample printout of FEREBA status information (section 5.2, page A5-3) as shown in figure 8. Also, the iteration approach discussed in section 5.0 is modified in the same manner as was discussed for the Theoretical Manual—Solution Methodology (section 2.1).

The discussion of convergence problems (section 5.3) is significantly modified by the new solution procedure. It remains true that for an iterative, nonlinear analysis such as that performed by FEREBA, absolute convergence cannot be guaranteed. The revised procedure, however, has greatly reduced the frequency of occurrence of nonconvergence with this program. The original approach required four iteration loops for a solution. The revised procedure eliminates the outer ring/carrier gap iteration loop and moves the force iteration outside the elastic deflection iteration. The possible errors associated with each of the three iteration loops are discussed in the following:

ERROR FROM DNEQNF—The number of calls to FCN has exceeded ITMAX\* (N+1).  
ERROR FROM DNEQNF—The iteration has not made good progress.

These errors are from the rolling element equilibrium iteration (DNEQNF is called from subroutine BRGFOR). The accuracy and iteration limits are initially set internally. The user-supplied accuracy and iteration limits for the shaft/inner race force iteration loop are substituted here if they call for a more precise solution (smaller accuracy, larger iteration limit). These values can be altered if this error occurs.

```

+-----+
R E B A N S - Rolling Element Bearing Analysis System - R E B A N S
+-----+

```

```

FFFFFFF  EEEEEEE  RRRRRR  EEEEEEE  BBBB  AAAA
FF        EE        RR  RR  EE        BB  BB  AA  AA
FFFFFFF  EEEEEEE  RRRRRR  EEEEEEE  BBBB  AAAAAA
FF        EE        RR  RR  EE        BB  BB  AA  AA
FF        EEEEEEE  RR    RR  EEEEEEE  BBBB  AA  AA

```

Flexibility Enhanced Rolling Element Bearing Analysis

Final Release Version 2.00 - Dated 01 August 1996

\*\*\*\*\*

Title Of Analysis Being Run:

Test Case with flexible outer ring, IBSCOR=2, 1 mil radial deadband

Name of Input Analysis File: /usr/people/ryansg/rebans/test1.dat

Name of Output Results File: test1s.out

\*\*\*\*\*

Forming Compliance Matrices for Outer Ring

reading previously reduced and inverted outer race file:

red.bor2ms3.asc

Compliance Matrices Created for Outer Ring, Elapsed Time = 0.41 secs

\*\*\*\*\*

Now Iterating to Determine Quasi-Static Equilibrium Solution

```

Elastic deformation iteration 1 complete, Error = 6.5675E+03%
Elastic deformation iteration 2 complete, Error = 2.0154E+07%
Elastic deformation iteration 3 complete, Error = 4.7745E+03%
Elastic deformation iteration 4 complete, Error = 4.6094E+05%
Elastic deformation iteration 5 complete, Error = 8.1675E+01%
Elastic deformation iteration 6 complete, Error = 1.0520E+01%
Elastic deformation iteration 7 complete, Error = 3.0943E-02%
Elastic deformation iteration 8 complete, Error = 9.6991E-05%
Elastic deformation iteration 9 complete, Error = 3.0534E-07%

```

Quasi-Static Iteration Finished - Elapsed Execution Time = 8.48 secs

\*\*\*\*\*

FEREBA Execution Completed, Total CP Time = 8.96 secs

Printed Output Written to File: test1s.out

\*\*\*\*\*

FIGURE 8.—Example of FEREBA status information output.



Activating print option level 3 will display the final iteration values. Option level 4 will display each value during the iteration process. The user can modify the action taken when these errors occur by enabling (uncommenting) the call to the routine ERSET. This call is made in the main program FEREBA. This will allow the user to test the value of the IMSL function IERCD after calling DNEQNF and specify action accordingly. Fortunately, the occurrence of these errors is the exception rather than the rule.

```
***** WARNING—Elastic deformations unconverged after ?? loops—WARNING *****
                                Error is = XXXXXXXXXX%
                                Requested maximum iteration error is = YYYYYYYYY%
***** WARNING—Solution may be acceptable—examine carefully—WARNING *****
```

This warning occurs in the elastic deflection iteration loop. If the solution is converging, the number of iterations allowed may be increased. If the error is small enough, the required accuracy may be increased. Activating print option level 2 will display information about gap constraint forces to aid in debugging, if necessary.

```
***** WARNING—Force iteration unconverged after ?? loops—WARNING *****
                                Error is = XXXXXXXXXX%
                                Requested maximum iteration error is = YYYYYYYYY%
***** WARNING—Solution may be acceptable—examine carefully—WARNING *****
```

This warning occurs in the force iteration loop. If the solution is converging, the number of iterations allowed may be increased. If the error is small enough, the required accuracy may be increased. Activating print option level 1 will display information about assumed inner race displacements and calculated inner race forces to aid in debugging, if necessary.

### **Additional User's Manual Changes**

The boundary conditions for outer race configuration 4 (illustrated on page 3–5) may not be representative of a user's configuration. It is not necessary to constrain the duplex bearing in the axial direction as shown. It must be restrained radially similarly to the primary bearing. While it is not necessarily erroneous to constrain the duplex bearing in the manner shown, it is not required as the text implies. The user should determine which constraints are appropriate for the configuration being analyzed.

## GENERAL COMMENTS ON ASSUMPTIONS AND INHERENT ERRORS

The assumptions required to formulate a mathematical representation of a physical device inevitably introduce errors. There are three particular errors of this nature in the REBANS analysis. Two of these are caused by the addition of race/support flexibility and the way it is modeled. The other error is not unique to this enhancement and probably exists in other bearing analysis programs.

The error that is not unique to REBANS is related to the summation of rolling element forces. When rolling element forces are summed on the inner race and the outer race, the two sums are not equal. This result is not physically possible. The difference is due to the neglect of rolling element azimuth angle deviations and tangential acceleration forces. In the classical quasi-static bearing analysis, the rolling element speeds are calculated based on the individual element kinematics (contact angles, etc.). In order for ball #1 to have a different orbital speed than ball #2, the ball must accelerate or decelerate in the tangential direction. The inertia force from this acceleration must be reacted on the raceways. In addition, the ball will make an excursion from the evenly spaced azimuth position usually assumed in the analysis. For a classical fixed outer race analysis, incorporating the acceleration forces and the azimuth angle deviations negates the difference in the sum of forces on the inner and outer races. This cannot be easily corrected in the REBANS analysis. The ball forces can only be applied at the fixed azimuth positions defined by the finite element model node locations. The present form of the program also reduces out tangential DOF's from the race model so that the acceleration forces cannot be applied. The magnitude of this error is on the order of 1–2 percent.

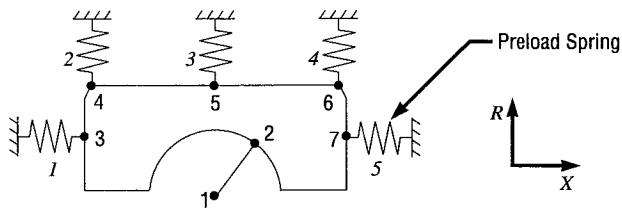
The two REBANS unique errors are related to the finite element model grid. The first of these is related to ball bearing contact angles. The ball/race contact loads must be applied to a fixed node location on the race. This point is typically placed at either the unloaded contact angle or the estimated loaded contact angle. The actual contact angles vary from ball to ball and will not, in general, equal the assumed value used to define the finite element model grid. While the loads are applied at the correct angle, their line of application is displaced slightly to match the node location. The magnitude of this error is difficult to quantify; however, an analysis of a rigid ring (including a tilt DOF) with the same error simulated resulted in 1–2 percent error.

The second REBANS unique error is related to race/support contact. The race contacts the support with circumferentially and axially distributed contact loads. These distributed loads are represented by discrete forces applied to the structures. In the circumferential direction, there are as many locations as rolling elements. In the axial direction, there are three locations. The placement of the axial locations will have a direct effect on the tipping moment which can be reacted at the race corner. Chamfering and local flexibilities will alter where the “effective” reaction force should be placed to most accurately represent the actual mechanics of this interaction. The axial spacing error has been greatly reduced by incorporating the additional radial master DOF for the outer race. The error due to circumferential spacing requires further analysis to determine the degree of spatial resolution required to adequately represent the race/support contact mechanics.



## APPENDIX

2. Single ball bearing, flexible outer ring with deadband, carrier assumed rigid (IBSCOR=2). This model is nonlinear due to deadband contact, which is dependent on ball loads applied to the outer race. There are 5 gaps between the outer ring and rigid housing, and at each azimuthal position, 7 master nodes are required. After reduction in FEREBA, 9 DOF's remain at each ball location (4 axial, 5 radial).



### Active DOF's

ANSYS  $21 \cdot n$  (X, Y, Z)

FEREBA  $9 \cdot n$  (X, R)

### Active Nodes (DOF's)

X: 1, 2, 3, 7 (1, 4, 7, 19)

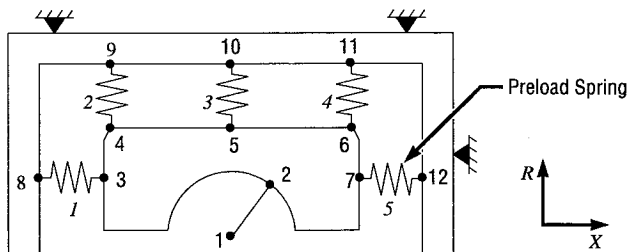
R: 1, 2, 4, 5, 6 (2, 5, 11, 14, 17)

### Reduced DOF's

3\*, 6, 8, 9, 10, 12, 13, 15, 16, 18, 20, 21

\* DOF 3 is deleted

3. Single ball bearing with flexible outer ring and carrier with deadband (IBSCOR=3). This model is nonlinear due to deadband contact, which is dependent on ball loads applied to the outer race, and also due to the preload spring (nodes 7-12), which can bottom. There are 5 gaps between the outer ring and carrier, and at each azimuthal position, 12 master nodes are required (7 on the outer ring, 5 on the carrier). After reduction in FEREBA, 14 DOF's remain at each ball location (6 axial, 8 radial).



### Active DOF's

ANSYS  $36 \cdot n$  (X, Y, Z)

FEREBA  $14 \cdot n$  (X, R)

### Active Nodes (DOF's)

X: 1, 2, 3, 7, 8, 12

(1, 4, 7, 19, 22, 34)

R: 1, 2, 4, 5, 6, 9, 10, 11

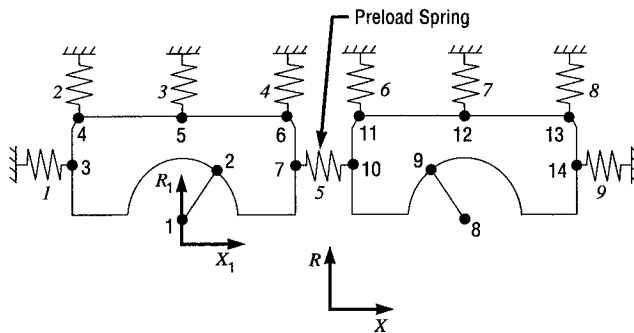
(2, 5, 11, 14, 17, 26, 29, 32)

### Reduced DOF's

3\*, 6, 8, 9, 10, 12, 13, 15, 16, 18, 20, 21, 23, 24, 25, 27, 28, 30, 31, 33, 35, 36

\* DOF 3 is deleted

5. Duplex ball bearing set with flexible outer rings with deadband and with carrier assumed rigid (IBSCOR=5). The analysis is restricted to having  $n$  equal in both bearings. This model is nonlinear due to deadband contact and the possibility that the preload spring (7–10) could bottom. There are 9 gaps between the outer ring and rigid housing, and at each azimuthal plane, 14 master nodes are required (7 on each bearing). After reduction in FEREB, 18 DOF's remain at each ball location (8 axial, 10 radial).



#### Active DOF's

ANSYS  $42 \cdot n$  (X, Y, Z)

FEREBA  $18 \cdot n$  (X, R)

#### Active Nodes (DOF's)

X: 1, 2, 3, 7, 8, 9, 10, 14

(1, 4, 7, 19, 22, 25, 28, 40)

R: 1, 2, 4, 5, 6, 8, 9, 11, 12, 13

(2, 5, 11, 14, 17, 23, 26, 32, 35, 38)

#### Reduced DOF's

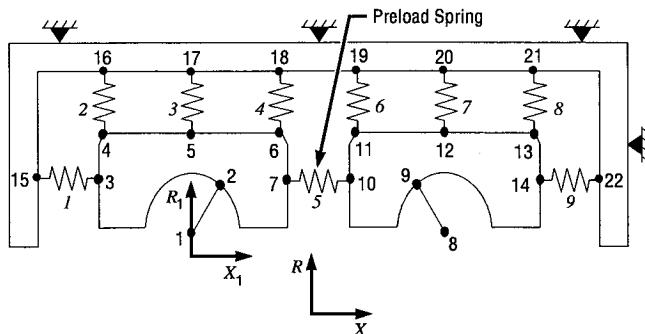
3\*, 6, 8, 9, 10, 12, 13, 15, 16, 18, 20, 21,

24\*, 27, 29, 30, 31, 33, 34, 36, 37, 39, 41, 42

\* DOF's 3 and 24 are deleted

The relative positions of the "primary" and "duplex" bearings are the same as configuration 4.

6. Duplex ball bearing set with flexible outer rings and carrier with deadband (IBSCOR=6). The analysis is restricted to having  $n$  equal in both bearings. This model is nonlinear due to deadband contact and the possibility that the preload spring (7–10) could bottom. There are 9 gaps between the outer ring and carrier, and at each azimuthal position, 22 master nodes are required (7 on each bearing and 8 on the carrier). After reduction in FEREB, 26 DOF's remain at each ball location (10 axial, 16 radial).



#### Active DOF's

ANSYS  $66 \cdot n$  (X, Y, Z)

FEREBA  $26 \cdot n$  (X, R)

#### Active Nodes (DOF's)

X: 1, 2, 3, 7, 8, 9, 10, 14, 15, 22 (1, 4, 7, 19, 22, 25, 28, 40, 43, 64)

R: 1, 2, 4, 5, 6, 8, 9, 11, 12, 13, 16, 17, 18, 19, 20, 21 (2, 5, 11, 14, 17, 23, 26, 32, 35, 38, 47, 50, 53, 56, 59, 62)

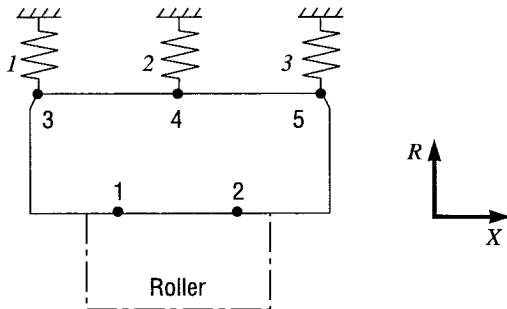
#### Reduced DOF's

3\*, 6, 8, 9, 10, 12, 13, 15, 16, 18, 20, 21,  
24\*, 27, 29, 30, 31, 33, 34, 36, 37, 39, 41,  
42, 44, 45, 46, 48, 49, 51, 52, 54, 55, 57, 58,  
60, 61, 63, 65, 66

\* DOF's 3 and 24 are deleted

The relative positions of the “*primary*” and “*duplex*” bearings are the same as configuration 4.

8. Cylindrical roller bearing with flexible outer ring with deadband and with carrier assumed rigid (IBSCOR=8). This model is nonlinear due to deadband contact. There are 3 gaps between the outer ring and rigid housing, and at each azimuthal position, 5 master nodes are required. After reduction in FEREBA, 5 radial DOF's remain at each roller location.



#### Active DOF's

ANSYS  $15 \cdot n$  (X, Y, Z)

FEREBA  $5 \cdot n$  (R)

#### Active Nodes (DOF's)

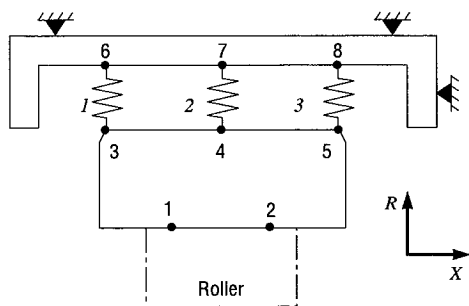
X: None

R: 1, 2, 3, 4, 5 (2, 5, 8, 11, 14)

#### Reduced DOF's

1, 3, 4, 6, 7, 9, 10, 12, 13, 15

9. Cylindrical roller bearing with flexible outer ring and carrier with deadband (IBSCOR = 9). This model is nonlinear due to deadband contact. There are 3 gaps between the outer ring and carrier, and at each azimuthal position, 8 master nodes are required (5 on the bearing and 3 on the carrier). After reduction in FEREBA, 8 radial DOF's remain at each roller location.



#### Active DOF's

RANSYS  $24 \cdot n$  (X, Y, Z)

FEREBA  $8 \cdot n$  (R)

#### Active Nodes (DOF's)

X: None

R: 1, 2, 3, 4, 5, 6, 7, 8  
(2, 5, 8, 11, 14, 17, 20, 23)

#### Reduced DOF's

1, 3, 4, 6, 7, 9, 10, 12, 13, 15, 16, 18, 19, 21,  
22, 24

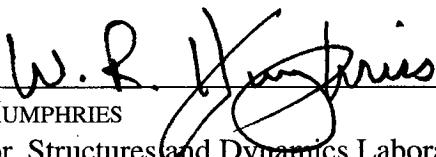


## **APPROVAL**

### **MODELING OF ROLLING ELEMENT BEARING MECHANICS— COMPUTER PROGRAM UPDATES**

Stephen Ryan

The information in this report has been reviewed for technical content. Review of any information concerning Department of Defense or nuclear energy activities or programs has been made by the MSFC Security Classification Officer. This report, in its entirety, has been determined to be unclassified.

  
\_\_\_\_\_  
W.R. HUMPHRIES  
Director, Structures and Dynamics Laboratory



|  |   |  |   |  |
|--|---|--|---|--|
| <b>REPORT DOCUMENTATION PAGE</b>   |   |  | Form Approved<br>OMB No. 0704-0188                                      |  |
| Public reporting burden for this collection of information is estimated to average 1 hour per response, including the time for reviewing instructions, searching existing data sources, gathering and maintaining the data needed, and completing and reviewing the collection of information. Send comments regarding this burden estimate or any other aspect of this collection of information, including suggestions for reducing this burden, to Washington Headquarters Services, Directorate for Information Operation and Reports, 1215 Jefferson Davis Highway, Suite 1204, Arlington, VA 22202-4302, and to the Office of Management and Budget, Paperwork Reduction Project (0704-0188), Washington, DC 20503   |   |  |   |  |
| 1. AGENCY USE ONLY (Leave Blank)   |   | 2. REPORT DATE<br>March 1997                               |   | 3. REPORT TYPE AND DATES COVERED<br>Technical Memorandum |
| 4. TITLE AND SUBTITLE<br>Modeling of Rolling Element Bearing Mechanics—<br>Computer Program Updates  |   |  | 5. FUNDING NUMBERS  |  |
| 6. AUTHORS<br>S.G. Ryan  |   |  |   |  |
| 7. PERFORMING ORGANIZATION NAME(S) AND ADDRESS(ES)<br>George C. Marshall Space Flight Center<br>Marshall Space Flight Center, Alabama 35812  |   |  | 8. PERFORMING ORGANIZATION<br>REPORT NUMBER                             |  |
| 9. SPONSORING/MONITORING AGENCY NAME(S) AND ADDRESS(ES)<br>National Aeronautics and Space Administration<br>Washington, DC 20546-0001  |   |  | 10. SPONSORING/MONITORING<br>AGENCY REPORT NUMBER<br><br>NASA TM-108532 |  |
| 11. SUPPLEMENTARY NOTES<br>Prepared by Structures and Dynamics Laboratory, Science and Engineering Directorate   |   |  |   |  |
| 12a. DISTRIBUTION/AVAILABILITY STATEMENT<br>Unclassified-Unlimited   |   |  | 12b. DISTRIBUTION CODE  |  |
| 13. ABSTRACT (Maximum 200 words)<br><br>The Rolling Element Bearing Analysis System (REBANS) extends the capability available with traditional quasi-static bearing analysis programs by including the effects of bearing race and support flexibility. This tool was developed under contract for NASA-MSFC. The initial version delivered at the close of the contract contained several errors and exhibited numerous convergence difficulties. The program has been modified in-house at MSFC to correct the errors and greatly improve the convergence. The modifications consist of significant changes in the problem formulation and nonlinear convergence procedures. The original approach utilized sequential convergence for nested loops to achieve final convergence. This approach proved to be seriously deficient in robustness. Convergence was more the exception than the rule. The approach was changed to iterate all variables simultaneously. This approach has the advantage of using knowledge of the effect of each variable on each other variable (via the system Jacobian) when determining the incremental changes. This method has proved to be quite robust in its convergence. This technical memorandum documents the changes required for the original Theoretical Manual and User's Manual due to the new approach. |   |  |   |  |
| 14. SUBJECT TERMS<br>rolling element, bearing, stiffness, deadband, flexible race, quasi-static  |   |  | 15. NUMBER OF PAGES<br>32   |  |
|  |   |  | 16. PRICE CODE<br>NTIS  |  |
| 17. SECURITY CLASSIFICATION<br>OF REPORT<br>Unclassified   | 18. SECURITY CLASSIFICATION<br>OF THIS PAGE<br>Unclassified | 19. SECURITY CLASSIFICATION<br>OF ABSTRACT<br>Unclassified | 20. LIMITATION OF ABSTRACT<br>Unlimited                                 |  |



National Aeronautics and  
Space Administration  
Code JTT  
Washington, DC  
20546-0001

*Official Business*  
*Penalty for Private Use, \$300*

*Postmaster: If Undeliverable (Section 158 Postal Manual), Do Not Return*

---